Cutaneous Wound Healing is Enhanced by Nrf2-Induced Expansion of Hair Follicle Stem Cell Populations

Semester Project 22.02.2016 – 27.05.2016

Andrina Stäubli, 12-929-022, andrinst@student.ethz.ch

Supervisor: PD Dr. Matthias Schäfer

Institute of Molecular Health Science

D-Biol, ETHZ

Abstract

The nuclear factor erythroid 2-like 2 (Nrf2) transcription factor plays an important role in the antioxidant response. High levels of reactive oxygen species, like during skin wound healing, activate Nrf2 and subsequently cytoprotective molecules.

Mice with a strong keratinocyte-specific upregulation of Nrf2 display a severe epidermal phenotype. Additionally to acanthosis and hyperkeratosis of the epidermis they also exhibit accelerated closure of full thickness skin wounds. In this project I could show that Nrf2 mediated activation of antioxidant pathways did not have an influence on the increase in the length and area of the wound epithelium. Nrf2 activation did also not lead to accelerated keratinocyte migration *in vitro*. Keratinocytes for wound re-epithelialization were shown to originate, among other, from different hair follicle stem cell populations. Mice overexpressing Nrf2 have an increased keratinocyte reservoir for re-epithelialization during wound healing due to the expansion of junctional zone and upper isthmus hair follicle stem cells as well as overall epidermal keratinocyte overproliferation. This increased proliferation in the epidermis and the hair follilce is mediated by Nrf2-induced epigen activation, which is an EGFR ligand.

Contents

List of Figures

List of Tables

1 Introduction

1.1 The murine skin and hair follicles

The skin plays a very important role as a protective barrier against environmental exposures, such as ultra violet (UV) radiation, invasive microbes, mechanical stresses and chemicals. It also prevents dehydration by limiting water loss to the air. This barrier is mostly maintained by the outermost layer of the skin, the epidermis, which lies above the mesenchymal dermis and hypodermis (subcutaneous fat). Keratinocytes inside the epidermis originate from stem cell niches in the basal lamina, which separates epidermis from dermis, and the basal layer. As the cells proliferate and terminally differentiate, they travel towards the surface of the skin through the suprabasal layers stratum spinosum, granulosum and corneum [1] (see Figure 1). During normal skin homeostasis terminally differentiated keratinocytes from the stratum corneum are continuously shed and replenished by new cells.

Other parts of the epidermis are skin appendages such as hair follicles (HF), sebaceous and sweat glands, that are anchored deep inside the dermis. Hair might serve as a heat protecti layer in the case of fur, or as additional sensory organs like whiskers. Th llicle consists of several compartments; the outer root sheath, which is contiguous with the interfollicular epidermis (IFE), the inner root shaft and the hair shaft [2]. Next to the HF lies the sebaceous gland, which provides the hair and skin with lubrication [3]. Mature HF undergo cycles of growth (anagen), regression (c gen) and rest (telogen) during homeostasis [2]. Actively dividing, relatively u ferentiated cells embedded in the matrix around the dermal papilla at the hair root produce the rod shaped hair follicle during the anagen phase of the hair cycle. During catagen, the l er part of the cycling HF regresses and the dermal papilla moves upward to ls the permanent upper part. After the telogen resting phase, the hair cycle begins again. A new follicle adjacent to the old hair is formed. As the old hair is shed, the new hair emerges from the same orfice [4].

The regeneration of the hair follicle requires a reservoir of multipotent stem cells (SC) that can be activated to form the new HF. These cells reside in the lowest part of the permanent HF called the bulge [5]. Bulge stem cells are slowly cycling, multipotent and express cluster of differentiation 34 (CD34) as well as keratin 15 (K15) [6]. The HF comprises many distinct stem cell populations that all contribute to the independent maintenance of their individual compartments. The isthmus above the bulge at the level of the sebaceous gland contains leucine-rich repeat containing G protein-coupled receptor 6 (Lgr6) and placenta expressed transcript 1 (Plet1) expressing stem cells. Leucine-rich repeats and immunoglobulin-like domains 1 (Lrig1) marked cells can be found in the upper part of the isthmus, the so-called junctional zone. Above that, the infundibulum connects the HF to the interfollicular epide . It is contiguous with the epidermis and expresses the interfollicular mark tem cell antigen 1 (Sca1). All these SC populations are capable of reconstituting the whole HF and IFE, but do not donate cells towards normal homeostasis. Their residence inside individual niches maintains the expression of markers and other characteristics like quiescence or proliferation rate [6, 3, 7, 8, 9] (see Figure 1).

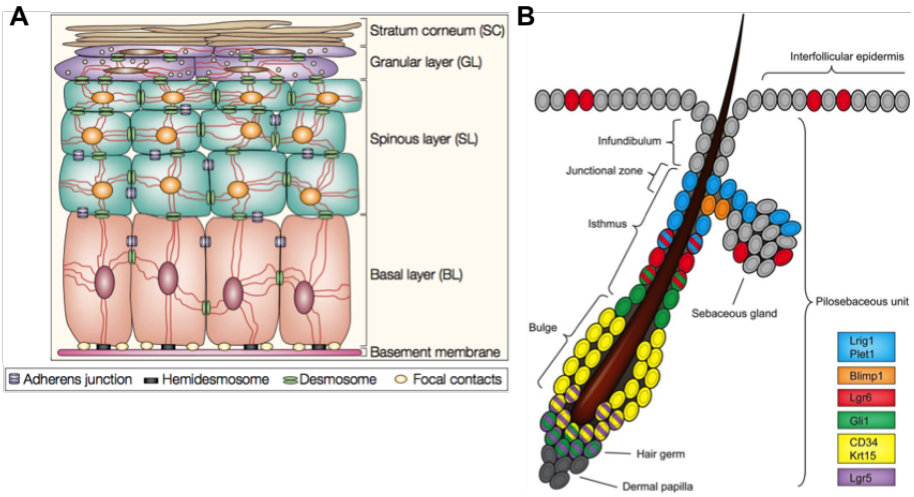

Figure 1: The skin and stem cells of the hair follicle.
A: Schematic representation of the different epidermal layers [1]. **B:** Schematic representation of the different stem cell populations in the hair follicle [3].

1.2 Wound healing

Cutaneous wounds interrupt the skins barrier and thus need to be repaired quickly. After wounding, a blood clot is formed to provisionally seal the open tissue and shield it from environmental stressors. Protection against invading pathogens is inferred by the infiltration of immune cells like neutrophils and later mast cells and monocytes, which differentiate into tissue macrophages [10]. In a process called the respiratory burst neutrophils and macrophages release toxic mediators such as reactive oxygen species (ROS) that eliminate contaminating bacteria, but can also attack resident tissue cells. Although ROS are crucial during this phase, elevated and sustained ROS leads to oxidative stress and a delayed healing process often seen in chronic wounds. Several exogenous and endogenous low molecular weight antioxidants and ROS-detoxifying enzymes are activated in response to increasing ROS concentrations [11, 12].

The second phase of wound healing is characterized by new tissue formation. Granulation tissue, consisting of migrated fibroblasts and massive amounts of extracellular matrix proteins, fills the wound. At the wound edge keratinocytes from the epidermis and the hair follicles migrate into the wound and start hyperproliferation to permanently re-epithelialize it. Some fibroblast differentiate into myofibroblasts responsible for wound contraction and deposition of additional matrix proteins. A few weeks after wounding, the grannulation tissue is slowly remodelled into mature scar tissue, which is a very dense connective tissue with reduced tensile strenght and elasticity [10].

1.3 Nrf2 – nuclear factor eryhtroid 2-like 2

The basic region-leucine zipper-type transcription factor nuclear factor erythroid 2-like 2 (Nrf2) is an important regulator of the antioxidant response. During

normal homeostasis under basal ROS levels, a Kelch-like ECH-associated protein 1 (Keap1) homodimer binds to Nrf2. Through interaction with the Cullin 3-based ubiquitin E3 ligase, Nrf2 is targeted for ubiquitination and proteosomal degradation. High ROS levels and oxidative stress can lead to the stabilization of Nrf2. Electrophilic reactions modify Keap1 cysteine residues and inactivate its ability to mediate E3 ligase activity. Unbound Nrf2 is then translocated to the nucleus where, together with small Maf proteins as cofactors, it binds to antioxidant response elements (ARE) in regulatory regions of several hundred target genes [13]. This initiates the transcription of cytoprotective genes like NAPD(H) dehydrogenase, quinone 1 (Nqo1), heme oxygenase (Ho-1) and the glutathion biosynthesis enzymes glutamate-cysteine ligase (regulatory and catalytic subunits: Gclm, Gclc), among others [14].

Numerous stress situations, such as UV radiation, xenobiotic toxins and wounding, induce increased ROS levels and thus activate Nrf2 and its target genes. Upon UVB irradiation differentiated keratinocytes of the suprabasal layers in the murine epidermis exhibit strong Nrf2 activity and thus protection from apoptosis. To prevent oxidative damage that could be passed on to the following generations, apoptosis due to ROS is preferred in stem cells. Thus Nrf2 expression and activity is lower in basal keratinocytes [15].

Activation of Nrf2 might strengthen the protective function of the skin , through its role in ROS detoxification. Nrf2-activating compounds, like the broccoli sprout extract sulforophane (SFN), have been shown to protect the skin from UV radiation induced apoptosis [16] and to improve the response to various environmental toxins [14]. Pharmacological Nrf2 activation might further infer some prophylaxis against cancer, but increased ROS detoxification was also shown also protect already existing tumor cellss [14].

During wound healing Nrf2 is particularly upregulated in the hyperproliferative wound epithelium. Although genetic deletion of Nrf2 does lead to a slightly delayed and prolongued expression of inflammatory cytokines, it does not alter the wound healing process otherwise [17]. Mouse models expressing dominant negative Nrf2 in their keratinocytes show no wound healing phenotype either, but the long-term reduced basal levels of ROS-detoxifying molecules increase the accumulation of oxidative damage and raises the animal's susceptibility to tumor formation [18]. Loss of Nrf2 activity seems only deleterious to the wound healing process under heightened stress situations. A diabetic mouse model with genetic Nrf2 deletion exhibited markedly delayed wound closure due to strongly increased oxidative stress and apoptosis. Pharmacological activation of Nrf2 could rescue the wound healing phenotype in the diabetic mice [19]. Contrary to this, neither pharmacological nor genetic activation of Nrf2 did improve the normal wound healing process [15, 14]. It can be assumed that Nrf2 activity during wound healing is only crucial during increased stress situations.

The effects of Nrf2 activity in keratinocytes was studied in a mouse model that expresses constitutively active Nrf2 (caNrf2) in keratinocytes. To induce overexpression of caNrf2, its coding sequence is placed before a cytomegalie virus (CMV) promoter in front of a β-actin promoter and followed by floxed STOP cassette. This is removed by cre recombinase under the control of a keratin 5 (K5) promoter, which is expressed only in basal keratinocytes [15, 20, 21]. The

resulting K5cre-CMVcaNrf2 mice have reduced size and weight, experience hair loss as well as dry and scaly skin. The strong epidermal phenotype is characterized by acanthosis and hyperkeratosis, meaning the thickening of the viable epidermis as well as the stratum corneum, the outermost layer of dead skin cells. A defect in their epidermal barrier and the following continuous inflammatory response most likely leads to the incrased expression of mitogens, which activates keratinocyte hyperproliferation [20]. Additionally, they display hyperproliferation and hyperkeratosis of hair follicles and sebaceous glands. Recently, epigen was reported to be a direct target of increased Nrf2 actvivity, through association of Nrf2 with an upstream ARE of epigen [22]. It seems at least partially responsible for activation of hyperproliferation by binding to Egfr and downstream Mapk signaling[23].

1.4 Project aim

K5cre-CMVcaNrf2 mice display significantly faster wound closure when compared to control mice. The aim of this project was to characterize skin wounds in K5cre-CMVcaNrf2 mice and improve the understading of the mechanism behind the accelerated wound healing phenotype. First, the influence of Nrf2 on migration was analyzed, followed by a closer look at the phenotype at the periphery of the wound, with a special focus on hair follicles and the Nrf2 target epigen.

2 Materials and methods

2.1 Animal experiments

2.1.1 Mouse model

Mice were kept under pathogen-free conditions in the ETH Phenomics Center (EPIC). All experiments were performed by an authorized person in the lab (M. Schäfer or S. Muzumdar) and approved by the local veterinary authorities of Zurich, Switzerland.

A mouse model with a genetic activation of Nrf2 in keratinocytes was established previously in the lab [20, 22]. Mice expressing the transgene Nrf2 under the control of the β-actin promoter with an upstream cytomegalie virus (CMV) enhancer were crossed with transgenic mice expressing Cre recombination under the K5 promoter [21]. This ensures that recombination is limited to keratinocytes and leads to an overexpression of constitutively active Nrf2 (K5cre-CMVcaNrf2).

2.1.2 Genotyping

Genotypes of mice were assessed by PCR. Genomic DNA from mouse ear skin clippings was extracted through the HotSHOT procedure. The skin samples were incubated in alkaline lysis buffer (25mM NaOH, 0.2mM EDTA [Axonlab, Baden, CH] in ddH2O) for a minimum of 20' at 95℃ and neutralized with an equal volume of neutralization buffer (40mM Tris-HCl in ddH2O). DNA was PCR amplified using the KAPA 2G Fast Genotyping kit with dye (KAPA Biosystems KK5121, Massachusetts, USA). For program used see Table 1 and for primers Table 3. The genotype was determined by running PCR products on a 1.5% agarose gel (2.7g agarose [Bio&Sell, Nuremberg, DE], 180ml 1x SBA buffer [20x SBA: 8g NaOH, 50g Boric Acid, 800ml ddH2O], 8µl EtBr [Fluka Bio-Chemika, Buchs, CH]) with a 100 bp DNA Marker (Bio&Sell, Nuremberg, DE).

Table 1 Cycling programs used for genotyping

Temp.	Time	Rep.	Temp.	Time	Rep.
Genotyping cre			**Genotyping caNrf2**		
110℃	heat lid		110℃	heat lid	
95℃	5' 0"		95℃	5' 0"	
95℃	30"	40x	95℃	30"	40x
53℃	15"	40x	61℃	15"	40x
72℃	5"	40x	72℃	5"	40x

2.1.3 Wounding

The wound healing process was analyzed with biopsies from full-thickness and abrasion wounds. 8-11 week old-old mice were used, with their hair in the telo-

gen phase of the hair cycle. Mice were anesthetized by inhalation of isofluorane (Isocare, Animal Care Ltd, York, UK) before wounding. Wound biopsies were taken after euthanization by CO_2 inhalation. For full-thickness wounds two anterior and posterior wounds lateral to the spine were made with a 5mm hole punch (Stiefel, Brentford, UK). The biopsies were harvested 3 or 5 days after wounding.

Abrasion wounds were created by removing the cornified, granular and spinous layers of the epidermis by tape stripping with 'Tesa Extra Power Perfect Tape' (Tesa tape Schweiz AG, Bergdietlikon, CH). For tg/wt (K5cre-wt) mice 15 tape strips were needed. To account for epidermal hyperkeratosis and acanthosis in tg/tg mice (K5cre-CMVcaNrf2) 25 strips were needed to achieve similar abrasion as in tg/wt. Tape stripped area were harvested 42h after wounding.

Total RNA for qPCR analysis was extracted from ultra-torraxed homogenized skin tissue biopsies by means of the phenol-chloroform extraction method.

2.2 Morphometrical analysis

Haematoxylin and Eosin (H&E, both Sigma, Munich, DE) stained 7µm paraffin (Sigma, Munich, DE) sections from acetic ethanol fixed tape stripping biopsies were digitally imaged. The images were analyzed for length of neo-epidermis, number of cells in neo-epidermis and distance between hair follicles with the OpenLab software (3.5.1, Improvision/ Perkin Elmer, Waltham, USA).

2.3 Immunohistochemistry

Cryo sections from wound biopsies were dried at RT before fixation in 1% PFA (Paraformaldehyde, Sigma, Munich, DE) in PBS (phosphate buffered saline, for 10X 137mM NaCl, 10mM Na_2HPO_4, 2.7mM KCl, 2mM KH_2PO_4, ddH_2) for 10'. Sections were blocked and primary antibody was applied over night at 4℃. Secondary antibody was applied for 1h at RT and slides were mounted using Mowiol mounting solution (4.8g Mowiol [Hoechst, Oftringen, CH], 8ml 95% glycerol [Schweizerhall Chemie AG, Basel, CH], 12ml ddH2O, 24ml 0.2M pH 8.5 Tris) supplemented with 1x DABCO (for 10x: 4.5g DABCO [Sigma-Aldrich, Steinheim, DE] in 15ml ddH2O). A list of antibodies used can be seen in table 4.

2.4 RNA isolation and qRT-PCR

RNA was purified using the RNeasy mini kit (Qiagen, Hilden, DE) and protocol. Concentration of RNA was determined using a NanoDrop Spectrophotometer (ND-1000, Witec AG, CH). Using the reverse transcriptase iScriptTM cDNA Synthesis kit (Bio-Rad, Reinach, CH), cDNA was prepared from 0.5µg purified RNA. qPCR of cDNA was performed for 50 cycles using a SYBR Green Lightcycler 480 (Roche, Basel, CH). See Table 2 for cycling program and 3 for primers used.

Table 2 Cycling progrms used for qRT-PCR

Temp.	Time	Rep.	Temp.	Time	Rep.
72℃	10' 0"		72℃	10' 0"	
cDNA synthesis			**qRT-PCR**		
25℃	5' 0"		95℃	10' 0"	
42℃	30' 0"		95℃	10"	50x
85℃	05' 0"		60℃	20"	50x
04℃	forever		72℃	20"	50x
			95℃	5"	
			65℃	1' 0"	
			95℃	5aq./℃	
			40℃	30"	

2.5 Cell culture

Immortalized murine keratinocytes (IMKs) were cultured in 3:1+ medium (defined keratinocytes SFM [Invitrogen, 10744-019, Zug, CH, supplemented with provided growth supplements, 1% penicillin/ streptomycin (P/S, Sigma P-0781, Munich, DE), 5µl 10^{-5} M cholera toxin (CT, Sigma C-8052, Munich, DE)] and MEM Eagle, Spinner modification [Sigma, M8167, Munich, DE, supplemented with 10mg/ml insulin, 5 mg/ml transferrin, 1.4 mg/ml phosphoetanolamine, 0.61mg/ml ethanolamine, 5ng/ml hydrocortisone, 2mM glutamine, 1% P/S, 8% chelated FCS, 45µM $CaCl_2$), and 1:1000 EGF]). Pharmacological activation of Nrf2 in IMKs was achieved by addition of 5mM sulforophane (SFN, Sigma-Aldrich, Steinheim, DE) or vehicle control (DMSO, Sigma-Aldrich, Steinheim, DE) over night. Epigen treatment was tested with concentrations of 0, 50, 100, 200 and 500 nM recombinant epigen in 3:1+ medium.

2.6 Migration assays

Scratch assays were performed on confluent IMKs treated with 5mM SFN over night or on primary keratinocytes harvested from transgenic mice. Scratches, to mimic a wound, were implemented with 200µl filtered pipette tips vertically in the middle of the well of a 6-well plate. Pictures were taken from the same area at 0h, 8h and 24h for the IMKs and at 0h, 18h and 96h for the primary keratinocytes. Cells inside the area of the scratch were counted using OpenLab software.

Transwell assays were performed using tissue-treated polycarbonate membrane inserts with 8µm pore size for 24-well plates (Corning Incorporated, 3422, Corning, USA). 10'000 IMKs were seeded onto membranes after overnight treatment with 5mM SFN. Membranes were harvested at four different time points (20' after seeding, 24h, 30h and 48h). Cells on membranes were fixed in 4% PFA for 20' and stained with Hoechst (1:1000) in PBS. Cells above and below membrane were counted from four different locations on each membrane using OpenLab software.

2.7 Western blotting

Cells were lysed using SDS Laemmli buffer (for 5X: 10% SDS [Sigma-Aldrich, Steinheim, DE], 250mM pH6.8 Tris-HCl, 50% glycerol, 0.5mg/ml bromophenol blue, 680µl β-mercaptoethanol [Sigma-Aldrich, Steinheim, DE]) and proteins were separated by SDS Page on a 10% acrylamide gel (for 4 resolving gels: 6.65ml 30% acrylamide [BioRad, Hercules, USA], 7.5ml pH8.8 1M Tris-HCl, 5.75ml ddH2O, 200µl 10% SDS, 85µl 20% APS [Sigma, Munich, DE], 10µl TEMED [Sigma-Aldrich, Steinheim, DE]; for stacking gel: 1ml stacking gel mix [53.4ml 30% acrylamide, 40ml 1M pH6.8 Tris, 216ml ddH_2O, 3.2ml 10% SDS], 1µl TEMED, 5µl 20% APS). Proteins were transferred onto nitrocellulose membranes by wet transfer. Membranes were blocked for 1h in 5% milk-TBST (5% dry milk powser [Rapidlait, migros, CH] in 1X TBS [10X TBS: 78.8g Tris base, 11.69g NaCl, ddH_2O to 1l, adjust tp pH7.5], 1% Tween-20 [Roth, Karlsruhe, DE]) at RT and primary antibodies was applied over night at 4°C. Secondary antibody-HRP was added for 1.5h at RT and staining was developed using luminol (Luminol A: 500µl 250mM luminol, 220µl 90mM coumaric acid, 5ml pH8.5 1M Tris-Cl, 45ml H_2O; Luminol B: 31µl 30% H_2O_2 [Meck, Darmstadt, DE], 5ml pH8.5 1M Tris-Cl, 45ml H_2O; mix 1:1). The antibodies used are listed in table 4.

2.8 Flow cytometry and sorting

Mice were euthanized by CO_2 inhalation and skin from abdomen and back was harvested. After subcutaneous fat removal, the skin was incubated in 3 U/ml dispase (Gibco by life techonologies, 17105-041, Godo Shuesi Co. Ltd, JP) and RPMI 1640 medium (Gibco by life technologies, 17400-025, Massachusetts, USA) for 45' at 37°C. The epidermis was separated from the rest of the skin with a scalpel and incubated in 0.2mg/ml DNase (Sigma, DN25-1G, Munich, DE) and 20µM $MgCl_2$ for 20' at RT on a shaker. To complete tissue dissociation EGTA and EDTA were added to a final concentration of 7.4mM and incubated for another 5'. To get a single cell suspension the dissolved tissue was filtered through 50µm cell strainers (Partec CellTrics, 04-0042-2317, Görlitz, DE). Cell surface staining was applied for at least 20' at 4°C. For a list of used antibodies see table 4. Cell populations were analyzed and sorted for different hair follicle stem cell populations in flow buffer (for 50ml: 1x PBS, 2% BSA [Sigma-Aldrich, Steinheim, DE], 3mM EGTA).

2.9 Statistical analysis

Statistical analysis was performed with a non-parametric Mann-Whitney U-test for non-Gaussian distributions. Error bars represent standard deviations (SD), significance levels are marked as follows: *$p \leq 0.05$, **$p \leq 0.01$. Prism software (Version 5, GraphPad Software, La Jolla, USA) was used for all analysis.

Table 3 Primers

Gene	Fwd Primer	Rev Primer
Genotyping		
caNrf2	CTTATTCAAGCGGCTTCCGC	CGGCTCAGCACCTTGTATC
Cre	TCATCAGCTACACC	AACATGCTTCATCGTCGG
qRT-PCR		
Gapdh	CACCACCCTGTTGCTGTAGCCGTAT	TCGTGGATCTGACGTGCCGCCTG
Gsta3	CAAGGCAGTCTTGGCTTCTC	CAGAGTCCGGAAGATTTGGA
Srxn1	CGGTGCACAACGTACCAAT	TTGATCCAGAGGACGTCGAT
Mmp9		
Tgf-β1		

Table 4 Antibodies

Name	Company	Dilution
Immunofluorescence		
Plet1	Nordic-MUbio, MUB1512P, Susteren, NL	1:100
Anti-rat Cy3	Jackson Immuno Research, Suffold, UK	1:200
Hoechst 33342	Sigma-Aldrich, Steinheim, Germany	1:500
Western blot		
EGFR 2232	Cell Signaling, Leiden, NL	1:1000
pEGFR 2234	Cell Signaling, Leiden, NL	1:1000
ERK1/2 9102	Cell Signaling, Leiden, NL	1:1000
pERK1/2 9101	Cell Signaling, Leiden, NL	1:1000
FACS		
CD45-PacBlue	BioLegend, San Diego, CA	1:400
CD49f-Biotin	BioLegend, San Diego, CA	1:500
Strep-BV711		1:800
CD34-APC	BD Bioscience, Alschwil, CH	1:300
Sca1-PE-Cy7	BioLegend, San Diego, CA	1:500
Fc block	BD Bioscience, Alschwil, CH	1:200
Zombie fixable L/D		1:800

3 Results and Discussion

3.1 Characterization of cutaneous wounds in animals with strong genetic activation of Nrf2

The influence of Nrf2 on wound healing was analyzed using a mouse model with a strong genetic activation of Nrf2 in keratinocytes. A floxed STOP cassette, in front of constitutively active Nrf2 (mutant caNrf2) under the control of a β-actin promoter with a strong CMV enhancer, is excised in basal keratinocytes by the expression of Cre recombinase under a K5 promoter [21, 20] (Figure 2A).

On top of a severe epidermal phenotype, K5cre-CMVcaNrf2 (tg/tg) transgenic mice [15, 20] also present with accelerated wound healing. Length, area and number of cells inside the wound epithelium are significantly higher when compared to K5cre-wt (tg/wt) control mice, leading to faster re-epithelialization [24].

Analysis of gene expression in transgenic mice showed strong up-regulation of Nrf2 targets like NAD(P)H dehydrogenase, quinone 1 (Nqo1), glutamate cysteine ligase catalytic subunit (Gclc) [24], glutathione S-transferase A3 (Gsta3) and sulfiredoxin 1 (Srxn1) (see Figure 2B-C) in both non-wounded skin and 5 days after cutaneous wounding. In a constitutively active but not overexpressing Nrf2 mouse model (K5cre-caNrf2) it was shown that these same genes are only mildly, but still significantly, upregulated. Wound closure was not accelerated in this model compared to control mice [20].

The lack of a wound healing phenotypes in $Nrf2^{-/-}$ [17] or dnNrf2 [18] mouse models together with this data suggests that Nrf2 is not necessary for normal wound healing, but can be helpful if overexpressed.

Similar conclusions were drawn in a study on diabetic wound healing, where Nrf2 activation was shown to be necessairy for wound healing in high stress situations like diabetes, but not during normal conditions [19]. The higher basal oxidative stress in diabetic tissue together with the additional stress during wounding caused a delay in the healing process that could be aggravated by Nrf2 knockout or reversed by pharmacological Nrf2 activation before wounding. Downregulation of transforming growth factor beta 1 (Tgf-β1) and upregulation of matrix metalloproteinase 9 (Mmp9) in wounds of diabetic mice seemed to play a role in delayed healing. This hypothesis is supported by the ability of pharmacological Nrf2 activation to restore *Tgf-β1* and *Mmp9* levels [19].

In wounds of K5cre-CMVcaNrf2 mice no significant up- or downregulation of either *Tgf-β1* or *Mmp9* was detected compared to control mice. But *Tgf-β1* expression in both transgenic and control mice was increased 5 days after wounding compared to normal skin (Figure 2D). Mmp9 expression was significantly reduced in unharmed tissue of tg/tg when compared to tg/wt mice, but levels in wounded skin were similar in both (Figure 2E).

Tgf-β1 is involved in many aspects of the wound healing process: it promotes the expression and deposition of ECM proteins and is involved in scar formation, among others [25]. The role of Tgf-β1 in the inflammatory phase of wound healing by recruitment of immune cells could link it to oxidative stress and ROS formation. Nrf2 does not seem to regulate Tgf-β1 in a non-diabetic background and thus ROS modulation is probably not the cause for the longer

wound epithelium in K5cre-CMVcaNrf2 mice.

The role of Mmp9 in wound healing is controversial. Some Mmp9 activity inside the wound is important for keratinocyte migration, as complete Mmp9 knockout is deleterious for wound closure, but increased activity can also inhibit keratinocyte proliferation [26]. The downregulation of Mmp9 by Nrf2 in the normal skin might, in part, be responsible for increased keratinocyte proliferation in the K5cre-CMVcaNrf2 mice. During wounding, Nrf2 seems to modulate *Mmp9* expression only under heightened stress situations, as normal Mmp9 levels are actually beneficial for wound closure.

Thus Tgf-β1 and Mmp9 regulation by Nrf2 do not seem to be the cause for accelerated wound healing in non-diabetic K5cre-CMVcaNrf2 mice.

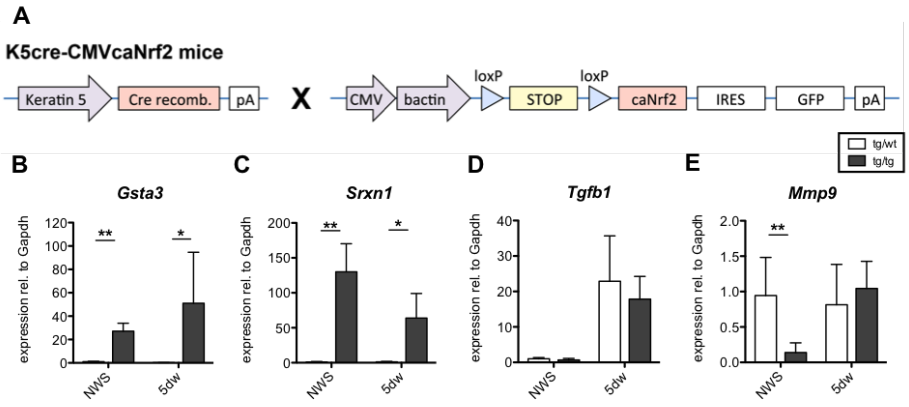

Figure 2: Cutaneous wound healing in K5cre-CMVcaNrf2 mice.
A: Schematic representation of K5cre-CMVcaNrf2 mouse model [20]. **B-E:** qRT-PCR of Nrf2 targets (B)*Gsta3*, (C) *Srxn1*, (D) *Tgfb1* and (E) *Mmp9* relative to *Gapdh*. RNA used was extracted form epidermis of non-wounded skin (NWS) and 5 days after wounding (5dW) of control (tg/wt) and K5cre-CMVcaNrf2 (tg/tg) mice. Mean values of non-wounded epidermis of tg/wt mice were arbitrarily set to 1. N=4-6. *P$\leq$0.05, **P$\leq$0.01. Mann-Whitney-U test.

3.2 Keratinocyte migration is not affected by pharmacological and genetic activation of Nrf2

Analysis of the wound epithelium in Nrf2-overexpressing mice revealed that although keratinocyte proliferation in unwounded skin was higher when compared to control mice, this was not the case at any stage after wounding [24]. Further, Nrf2 activation did not lead to decreased apoptosis [24], as it was suggested in the diabetic wound healing model by Long et al [19].

The effect of Nrf2 activation on keratinocyte migration was investigated by scratch- and transwell assay experiments. Neither pharmacological nor genetic Nrf2 activation did significantly alter keratinocyte migration in the scratch assays (Figure 3A-D). The migration of immortalized murine keratinocytes (IMKs), as analyzed by transwell assays, seems even slightly faster if Nrf2 is not pharmacologically activated. Cells with activated Nrf2 show linear increase of cells inside the scratch, whereas vehicle IMKs need more time to activate

migration, but then migrate faster (Figure 3E). In the second experiment total cell numbers were lower compared to the first, but migration did not seem to be affected by Nrf2 activation, except in the first time point (Figure 3F).

Nrf2 activation does not seem to affect keratinocyte migration, even if it is strongly overexpressed. It might be possible that Nrf2 has impact on keratinocyte migration in a different background or under more severe oxidative stress conditions.

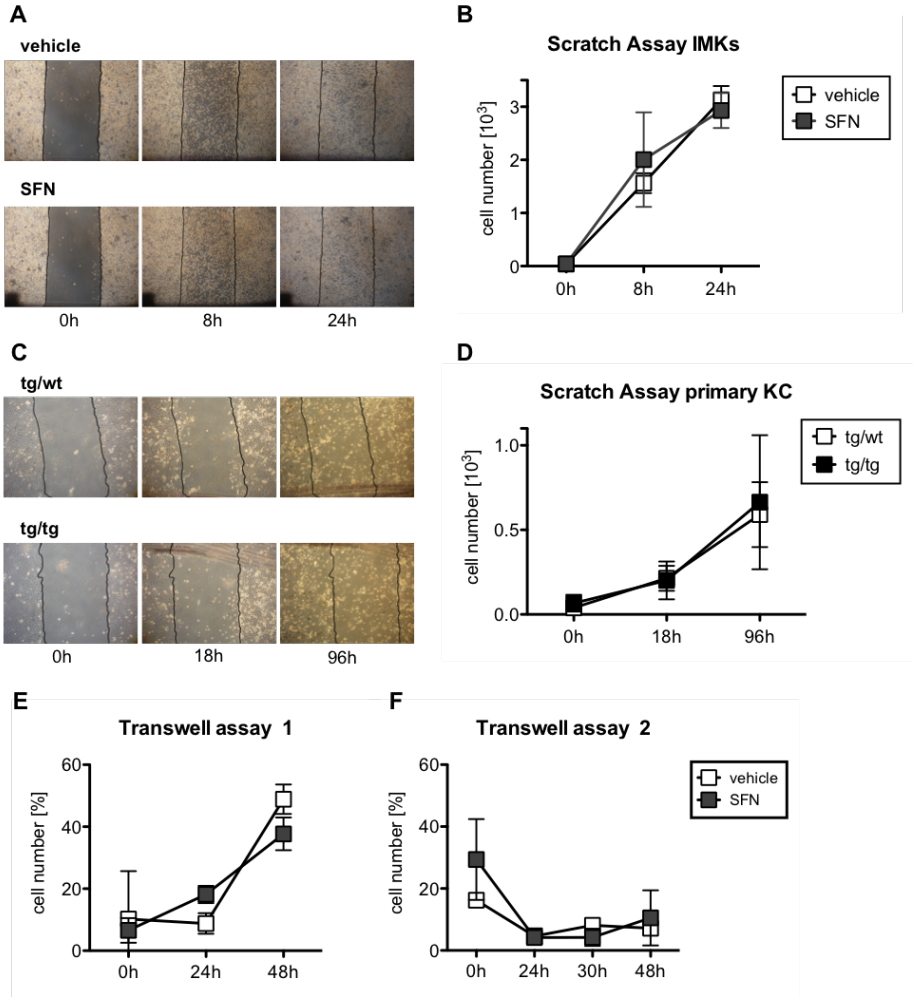

Figure 3: Effect of Nrf2 on *in vitro* keratinocyte migration.
A-B: Scratch assays with immortalized murine keratinocytes (IMKs) and pharmacological Nrf2 activation through overnight treatment with sulforophane (SFN). Total cell number inside the scratch was counted at timepoints 0h, 8h and 24h. N=6. **C-D:** Scratch assays with primary keratinocytes from control (tg/wt) and K5cre-CMVcaNrf2 (tg/tg) mice. Again total cell number inside the scratch was counted. N=3-6. **E-F:** Transwell assays with IMKs and pharmacological Nrf2 activation. Percentage of cell that migrated through a membrane with 8µm pores. N=4-5.

3.3 Abrasion wounds are re-epithelialized by keratinocyte migration from hair follicles

There seems to be no major difference between the wound tissues of K5cre-CMVcaNrf2 and control mice. Neither enhanced keratinocyte proliferation and decreased apoptosis inside the wound, nor faster migration from outside the wound contribute to the accelerated re-epithelialization phenotype of K5cre-CMVcaNrf2 mice. Outside of the wound the outer thickened epithelium is significantly increased in thickness and keratinocyte proliferation. Especially the hair follicles in the wound periphery display increased thickness, proliferation and Keratin 6 (K6) positive cells [24]. Wounding induces K6 expression in migrating and hyperproliferative keratinocytes of the outer root sheath in the hair follicle [27]. Cells originating from mostly quiescent stem cell pools in hair follicles have been reported as important sources for wound re-epithelialization [28].

To investigate whether keratinocytes from these altered hair follicles contribute to the faster wound closure of K5cre-CMVcaNrf2 mice, abrasion wounds were examined. The outer, differentiated layers of the epidermis, namely cornified, granular and spinous layers, were removed with tape (Figure 4A) and the neo-epidermis under the formed scab was morphometrically analyzed. Re-epithelialization seemed to originate from the hair follicles inside the abraded zone (Figure 4B). Formation of neo-epidermis between hair follicles in K5cre-CMVcaNrf2 was faster than in control mice, as a result of enhanced wound epithelium length and number of keratinocytes. Interestingly, the interfollicular length, meaning the average distance between hair follicles, was not increased in the Nrf2 overexpressing mice (Figure 4C-F).

The increased size of the interfollicular space and hair follicles in K5cre-CMVcaNrf2 mice, due to increased keratinocyte proliferation, serves as a plentiful source of keratinocytes during wound re-epithelialization. Especially cells from the hair follicles seem crucial for the wound healing process.

3.4 Genetic activation of Nrf2 leads to expansion of hair follicle stem cell populations in normal skin and proximal to the wound

There are at least three distinct stem cell populations (see Figure 5A) inside the hair follicle that contribute to re-epithelialization during wounding [29]. Stem cells from the junctional zone (JZ), upper isthmus (UI) and bulge region (BU) are capable to reconstitute the whole epidermis, including hair follicle and interfollicular space [6]. Flow cytometric analysis of epidermal cells from K5cre-CMVcaNrf2 mice revealed increased numbers and proliferation of cells from the junctional zone and upper isthmus, but not the bulge region. These results were confirmed by immunohistological stainings with leucine-rich repeats and immunoglobulin-like domains 1 (Lrig1), a marker for JZ, and placenta expressed transcript 1 (Plet1), a marker for UI, that showed the expansion of these stem cell populations. BU stem cell populations were not enlarged, as shown by keratin 15 (K15) stainings [24].

For further characterization the stem cell populations were flow-sorted and

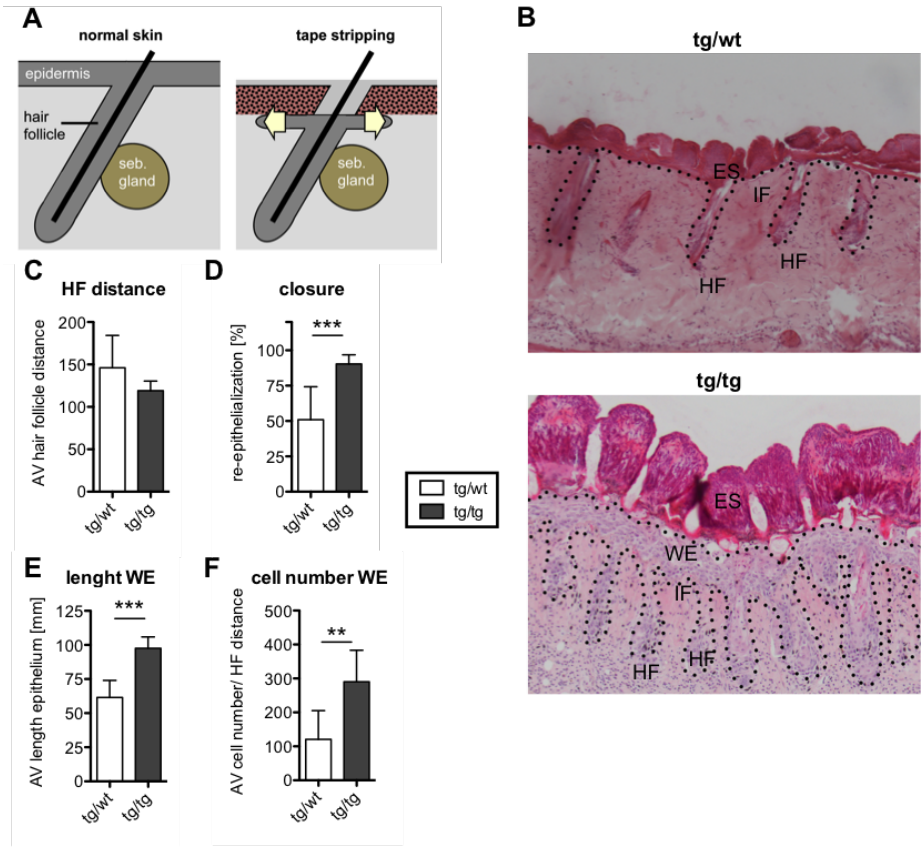

Figure 4: Abrasion wounds in K5cre-CMVcaNrf2 mice.
A: Schematic representation of abrarasion wound. Cornified, granular and spinous layers are removed with tesa tape strips. Formation of neo-epidermis between hair follicles [24]. **B:** H&E staining of tape stripped tg/wt and tg/tg mice 42h after wounding. Showing hair follicles (HF) and neo-epidermis (WE) in interfollicular space (IF) under the eschar (ES).
C-F: Morphological analysis of tape stripped mice. Showing (C) distance between hair follicles, (D) percentace of wound closure, (E) length of neo-epidermis and (F) number of keratinocytes inside the wound. N=6-9. *P≤0.05, **P≤0.01, ***P≤0.001. Mann-Whitney-U test.

the expression of markers indicative for specific sup-populations were analyzed. Hair follicle stem cells are stem cell antigen 1 (Sca1, a marker for interfollicular epidermis) negative and α6-integrin positive. UI stem cells express low levels of α6, whereas BU and JZ stem cells show high levels of α6. They can further be distinguished by the expression of cluster of differentiation 34 (CD34), which is present in BU but not in JZ cells [6, 9]. However, the results did not correspond with the expectations. Junctional zone cells are assumed to be *Lrig1* and *c-myc* positive (Figure 5B), whereas upper isthmus cells should be only *Plet1* positive (Figure 5C). Bulge region stem cells are usually characterized by (*CD34*) and leucine-rich repeat-containing G-protein coupled receptor 5 (*Lgr5*) expression (Figure 5D). Especially the low expression of *CD34* in BU stem cells, and its high expression in one of the UI stem cell populations is disconcerting, as the

cells were sorted for with a CD34-antibody. Since the flow sorting did not yield a very high cell quantity, it was difficult to extract sufficient amounts of RNA to perform qRT-PCR. Efforts to culture the sorted cells were also futile. It is furthermore possible, that the flow sorting strategy did not result in the desired cell populations, but this seems unlikely as a very similar process has been validated by Jensen et al [9].

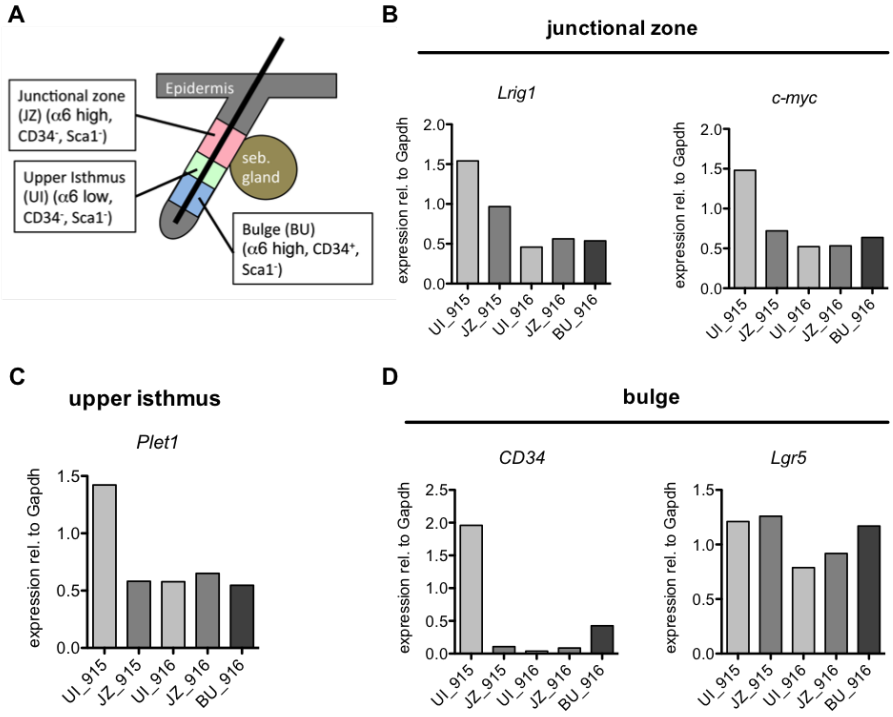

Figure 5: Hair follicle stem cell populations in K5cre-CMVcaNrf2 mice.
A: Schematic representation of three stem cell populations junctional zone (JZ), upper isthmus (UI) and bulge (BU) in murine hair follicles [24]. **B-D:** Epidermal cells of two control (tg/wt) mice (915, 916) were flow sorted. qRT-PCR of markers for (B) JZ (*Lrig1* and *c-myc*), for (C) UI (*Plet1*) and for (D) BU stem cells (*CD34* and *Lgr5*) relative to *Gapdh*.

The closer inspection of JU, UI and BU stem cell populations via flow cytometry confirmed enlarged cell populations and increased proliferation of JZ and UI stem cells also during wounding. Furthermore, Lrig1 fluorescence stainings revealed enlarged hair follicles proximal to the wound. Interestingly, the first two follicles closest to the wound show a marked reduction of Lrig1 staining [24]. Lrig1 is a negative regulator of proliferation. It inhibits epidermal growth factor receptor (Egfr) and subsequent mitogen-activated protein kinase (Mapk) signaling. Knock down of Lrig1 was shown to increase growth rate and cell population size [30]. Downregulation of Lrig1 in the first few hair follicles at the wound edge could be a way to increase proliferation and enlarge the keratinocyte pool for re-epithelialization of the wound. In accordance with this theory are the increased numbers of proliferating cell nuclear antigen (PCNA) positive cells in

these most proximal hair follicles, where Lrig1 expression is decreased (Figure 6A).

The expression of Plet1 in the first proximal hair follicle appears reduced too, as can be seen in immunofluorescence stainings (Figure 6B-C). This is surprising, since Plet1 downregulation was shown to have a negative effect on keratinocyte migration. Plet1 modulates cell adhesion and is usually strongly expressed at the leading wound edge or in suprabasal keratinocytes in contact with eschar [8]. One explanation for this downregulation of Plet1 could simply be that many of the Plet1 positive cells have already migrated into the wound at this stage of healing (day 5 after wounding).

Keratinocytes from the hair follicle, more specifically the junctional zone and upper isthmus stem cell populations, are present in increased numbers in K5cre-CMVcaNrf2. They appear to be crucial as an expanded reservoir of keratinocytes to re-epithelialize the wound and offer a plausible explanation for the faster wound closure in these mice.

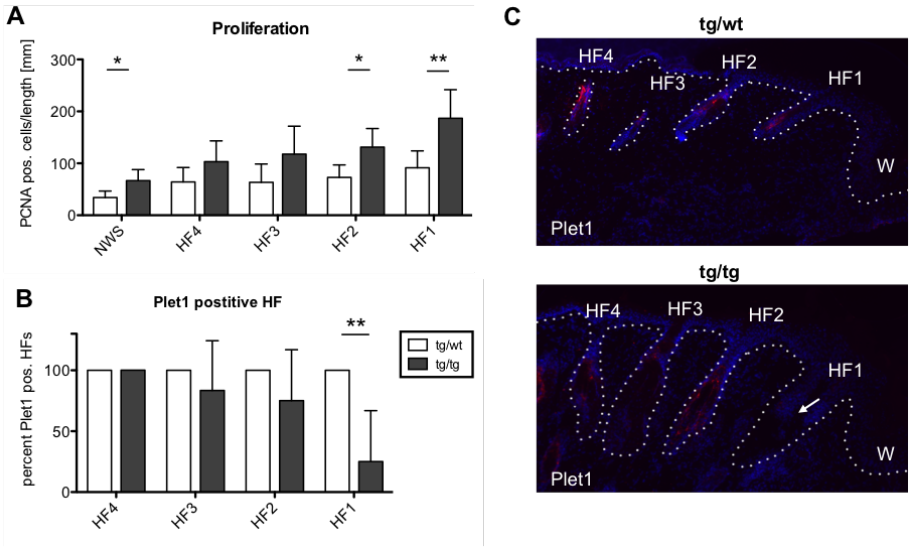

Figure 6: Hair follicle stem cells in the wound periphery of K5cre-CMVcaNrf2 mice.
A: Proliferating cell nuclear antigen (PCNA) positive cells in non wounded skin (NWS) and in the first 4 hair follicles (HF) at the wound edge. N=3-7. *P≤0.05, **P≤0.01, ***P≤0.001. Mann-Whitney-U test. **B:** Percent Plet1 positive hair follicles proximal to tg/wt and tg/tg wounds. N=6-8. **C:** Immunofluorescence staining of Plet1 in the first 4 hair follicles (HF) at the wound (W) edge 5 days after wounding of tg/wt and tg/tg mice. Arrow indicates markedly reduced Plet1 staining.

3.5 Epigen might be the driving force behind the expanded hair follicles

Epigen was recently shown to be a target of Nrf2 by Schäfer et al. [22]. It stimulates proliferation of cells through EGFR activation and the MAPK signaling pathway [23]. Additionally to being upregulated in non wounded skin, epigen

expression was increased 1 and 3 days after wounding in K5cre-CMVcaNrf2 mice [24]. To confirm the effect of epigen on keratinocyte proliferation, IMKs were treated with recombinant epigen over night and subsequent activation of Egfr and Erk1/2 (Mapk) was tested (Figure 7A). However, activation of Mapk (phospho-Erk1/2) appeared greater in untreated cells compared to any epigen concentration administered. This could be due to the fact that the cells were not starved before treatment as is required for epigen activation. The Egfr antibody staining did not reveal any bands of the expected size (175kDa), even though antibodies were tested for western blot. This might be due to a problem with the protein extraction method, as tests were done on proteins extracted by lysis buffer and not just SDS loading dye.

Nevertheless, the upregulation of epigen in the wound tissue points in the direction of epigen as the link between Nrf2 and the increased proliferation of JZ and UI stem cells. The working model by Muzumdar et al. [24] proposes Nrf2 induced activation of epigen, which in turn activates Egfr and Mapk signaling in the JZ and UI stem cells. This increased keratinocyte population in the hair follicle then is responsible for a fast and efficient re-epithelialization of the wound in K5cre-CMVcaNrf2 mice (Figure 7B).

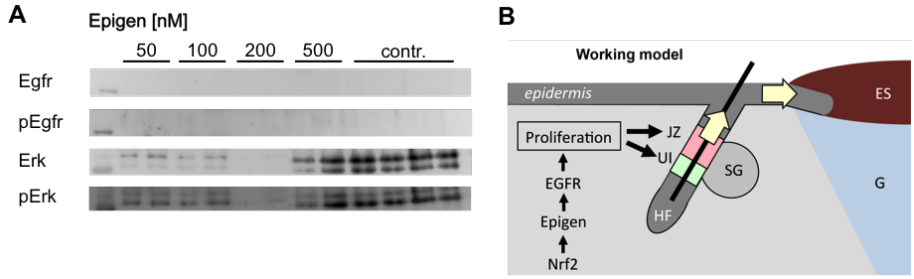

Figure 7: Nrf2 and epigen expression in K5cre-CMVcaNrf2 mice.
A: Western blot of . proteins from IMKs treated with 50 to 500 nM recombinant epigen stained for presence of Efgr, pEfgr, Erk and pErk. Cells were not starved before over night treatment. **B:** Schematic representation of current working model. Nrf2 activates epigen, which leads to Egfr and Mapk signaling. The following increased junctional zone (JZ) and upper isthmus (UI) stem cell proliferation in the hair follicle (HF) is cruicial for fast re-epithelialization of wounds. SG = sebaceous gland, ES = eschar, G = granulation tissue [24].

Acknowledgment

I would like to thank PD Dr. Matthias Schäfer for the opportunity to participate in this research project, as well as for his guidance and support. I am very grateful to Sukalp Muzumdar and Hailey Hiebert for their counsel and help with the experimental work. I would like to extend my gratitude to all the students who worked on this project before me: Andreas Bapst, Jonas Schwestermann and Alessia Gravina. Lastly, I'd like to thank the whole Werner group and Prof. Dr. Sabine Werner.

References

[1] Elaine Fuchs and Srikala Raghavan. Getting under the skin of epidermal morphogenesis. *Nat Rev Genet*, 3(3):199–209, Mar 2002.

[2] María Eugenia Balañá, Hernán Eduardo Charreau, and Gustavo José Leirós. Epidermal stem cells and skin tissue engineering in hair follicle regeneration. *World journal of stem cells*, 7(4):711, 2015.

[3] Troels Schepeler, Mahalia E Page, and Kim B Jensen. Heterogeneity and plasticity of epidermal stem cells. *Development*, 141(13):2559–67, Jul 2014.

[4] Laura Alonso and Elaine Fuchs. The hair cycle. *J Cell Sci*, 119(Pt 3):391–3, Feb 2006.

[5] Gina Taylor, Michael S Lehrer, Pamela J Jensen, Tung-Tien Sun, and Robert M Lavker. Involvement of follicular stem cells in forming not only the follicle but also the epidermis. *Cell*, 102(4):451–461, 2000.

[6] Viljar Jaks, Maria Kasper, and Rune Toftgård. The hair follicle—a stem cell zoo. *Experimental cell research*, 316(8):1422–1428, 2010.

[7] Mahalia E Page, Patrick Lombard, Felicia Ng, Berthold Göttgens, and Kim B Jensen. The epidermis comprises autonomous compartments maintained by distinct stem cell populations. *Cell Stem Cell*, 13(4):471–482, 2013.

[8] Karine Raymond, Anja Richter, Maaike Kreft, Evelyne Frijns, Hans Janssen, Monique Slijper, Silke Praetzel-Wunder, Lutz Langbein, and Arnoud Sonnenberg. Expression of the orphan protein plet-1 during trichilemmal differentiation of anagen hair follicles. *J Invest Dermatol*, 130(6):1500–13, Jun 2010.

[9] Kim B Jensen, Charlotte A Collins, Elisabete Nascimento, David W Tan, Michaela Frye, Satoshi Itami, and Fiona M Watt. Lrig1 expression defines a distinct multipotent stem cell population in mammalian epidermis. *Cell Stem Cell*, 4(5):427–39, May 2009.

[10] Matthias Schäfer and Sabine Werner. Cancer as an overhealing wound: an old hypothesis revisited. *Nat Rev Mol Cell Biol*, 9(8):628–38, Aug 2008.

[11] Matthias Schäfer and Sabine Werner. Oxidative stress in normal and impaired wound repair. *Pharmacol Res*, 58(2):165–71, Aug 2008.

[12] Christopher Dunnill, Thomas Patton, James Brennan, John Barrett, Matthew Dryden, Jonathan Cooke, David Leaper, and Nikolaos T Georgopoulos. Reactive oxygen species (ros) and wound healing: the functional role of ros and emerging ros-modulating technologies for augmentation of the healing process. *Int Wound J*, Dec 2015.

[13] Takafumi Suzuki and Masayuki Yamamoto. Molecular basis of the keap1–nrf2 system. *Free Radical Biology and Medicine*, 88:93–100, 2015.

[14] Matthias Schäfer and Sabine Werner. Nrf2—a regulator of keratinocyte redox signaling. *Free Radical Biology and Medicine*, 88:243–252, 2015.

[15] Matthias Schäfer, Sabine Dütsch, Ulrich auf dem Keller, Fatemeh Navid, Agatha Schwarz, Delinda A Johnson, Jeffrey A Johnson, and Sabine Werner. Nrf2 establishes a glutathione-mediated gradient of uvb cytoprotection in the epidermis. *Genes Dev*, 24(10):1045–58, May 2010.

[16] Konrad Kleszczyński, Insa MA Ernst, Anika E Wagner, Nathalie Kruse, Detlef Zillikens, Gerald Rimbach, and Tobias W Fischer. Sulforaphane and phenylethyl isothiocyanate protect human skin against uvr-induced oxidative stress and apoptosis: role of nrf2-dependent gene expression and antioxidant enzymes. *Pharmacological research*, 78:28–40, 2013.

[17] Susanne Braun, Christine Hanselmann, Marcus G Gassmann, Ulrich auf dem Keller, Christiane Born-Berclaz, Kaimin Chan, Yuet Wai Kan, and Sabine Werner. Nrf2 transcription factor, a novel target of keratinocyte growth factor action which regulates gene expression and inflammation in the healing skin wound. *Molecular and cellular biology*, 22(15):5492–5505, 2002.

[18] Ulrich auf dem Keller, Marcel Huber, Tobias A Beyer, Angelika Kümin, Christina Siemes, Susanne Braun, Philippe Bugnon, Varvara Mitropoulos, Delinda A Johnson, Jeffrey A Johnson, Daniel Hohl, and Sabine Werner. Nrf transcription factors in keratinocytes are essential for skin tumor prevention but not for wound healing. *Mol Cell Biol*, 26(10):3773–84, May 2006.

[19] Min Long, Montserrat Rojo de la Vega, Qing Wen, Manish Bharara, Tao Jiang, Rui Zhang, Shiwen Zhou, Pak K Wong, Georg T Wondrak, Hongting Zheng, and Donna D Zhang. An essential role of nrf2 in diabetic wound healing. *Diabetes*, 65(3):780–93, Mar 2016.

[20] Matthias Schäfer, Hany Farwanah, Ann-Helen Willrodt, Aaron J Huebner, Konrad Sandhoff, Dennis Roop, Daniel Hohl, Wilhelm Bloch, and Sabine Werner. Nrf2 links epidermal barrier function with antioxidant defense. *EMBO Mol Med*, 4(5):364–79, May 2012.

[21] Angel Ramirez, Angustias Page, Alberto Gandarillas, Jennifer Zanet, Sophie Pibre, Miguel Vidal, Laura Tusell, Anna Genesca, Duncan A Whitaker, David W Melton, and Jose L Jorcano. A keratin k5cre transgenic line appropriate for tissue-specific or generalized cre-mediated recombination. *Genesis*, 39(1):52–7, May 2004.

[22] Matthias Schäfer, Ann-Helen Willrodt, Svitlana Kurinna, Andrea S Link, Hany Farwanah, Alexandra Geusau, Florian Gruber, Olivier Sorg, Aaron J Huebner, Dennis R Roop, Konrad Sandhoff, Jean-Hilaire Saurat, Erwin Tschachler, Marlon R Schneider, Lutz Langbein, Wilhelm Bloch, Hans-Dietmar Beer, and Sabine Werner. Activation of nrf2 in keratinocytes causes chloracne (madish)-like skin disease in mice. *EMBO Mol Med*, 6(4):442–57, Apr 2014.

[23] Marlon R Schneider and Yosef Yarden. Structure and function of epigen, the last egfr ligand. In *Seminars in cell & developmental biology*, volume 28, pages 57–61. Elsevier, 2014.

[24] Skalp Muzumdar, Hayley Hiebert, Eric Haertel, Wilhelm Bloch, Sabine Werner, and Matthias Schäfer. Nrf2 activation enhances cutaneous wound healing by expansion of hair follicle stem cell populations. *Unpublished*, 2016.

[25] Mohammadreza Pakyari, Ali Farrokhi, Mohsen Khosravi Maharlooei, and Aziz Ghahary. Critical role of transforming growth factor beta in different phases of wound healing. *Advances in wound care*, 2(5):215–224, 2013.

[26] Vera L Martins, Matthew Caley, and Edel A O'Toole. Matrix metalloproteinases and epidermal wound repair. *Cell and tissue research*, 351(2):255–268, 2013.

[27] Sonja M Wojcik, Donnie S Bundman, and Dennis R Roop. Delayed wound healing in keratin 6a knockout mice. *Molecular and cellular biology*, 20(14):5248–5255, 2000.

[28] David M Ansell, Jennifer E Kloepper, Helen A Thomason, Ralf Paus, and Matthew J Hardman. Exploring the "hair growth-wound healing connection": anagen phase promotes wound re-epithelialization. *J Invest Dermatol*, 131(2):518–28, Feb 2011.

[29] Maksim V Plikus, Denise L Gay, Elsa Treffeisen, Anne Wang, Rarinthip June Supapannachart, and George Cotsarelis. Epithelial stem cells and implications for wound repair. In *Seminars in cell & developmental biology*, volume 23, pages 946–953. Elsevier, 2012.

[30] Kim B Jensen and Fiona M Watt. Single-cell expression profiling of human epidermal stem and transit-amplifying cells: Lrig1 is a regulator of stem cell quiescence. *Proc Natl Acad Sci U S A*, 103(32):11958–63, Aug 2006.

Eidgenössische Technische Hochschule Zürich
Swiss Federal Institute of Technology Zurich

Eigenständigkeitserklärung

Die unterzeichnete Eigenständigkeitserklärung ist Bestandteil jeder während des Studiums verfassten Semester-, Bachelor- und Master-Arbeit oder anderen Abschlussarbeit (auch der jeweils elektronischen Version).

Die Dozentinnen und Dozenten können auch für andere bei ihnen verfasste schriftliche Arbeiten eine Eigenständigkeitserklärung verlangen.

Ich bestätige, die vorliegende Arbeit selbständig und in eigenen Worten verfasst zu haben. Davon ausgenommen sind sprachliche und inhaltliche Korrekturvorschläge durch die Betreuer und Betreuerinnen der Arbeit.

Titel der Arbeit (in Druckschrift):

Verfasst von (in Druckschrift):
Bei Gruppenarbeiten sind die Namen aller Verfasserinnen und Verfasser erforderlich.

Name(n):	**Vorname(n):**

Ich bestätige mit meiner Unterschrift:
- Ich habe keine im Merkblatt „Zitier-Knigge“ beschriebene Form des Plagiats begangen.
- Ich habe alle Methoden, Daten und Arbeitsabläufe wahrheitsgetreu dokumentiert.
- Ich habe keine Daten manipuliert.
- Ich habe alle Personen erwähnt, welche die Arbeit wesentlich unterstützt haben.

Ich nehme zur Kenntnis, dass die Arbeit mit elektronischen Hilfsmitteln auf Plagiate überprüft werden kann.

Ort, Datum	**Unterschrift(en)**

Bei Gruppenarbeiten sind die Namen aller Verfasserinnen und Verfasser erforderlich. Durch die Unterschriften bürgen sie gemeinsam für den gesamten Inhalt dieser schriftlichen Arbeit.